



DNA 4240F

IONOSPHERIC IRREGULARITIES: OPTICAL SUPPORT OF HAES SCINTILLATION EXPERIMENTS

Lockheed Palo Alto Research Laboratory 3251 Hanover Street Palo Alto, California 94304

31 January 1977

Final Report for Period 15 December 1975-31 January 1977

CONTRACT No. DNA 001-76-C-0182

APPROVED FOR PUBLIC RELEASE; DISTRIBUTION UNLIMITED.

THIS WORK SPONSORED BY THE DEFENSE NUCLEAR AGENCY UNDER RDT&E RMSS CODE B322076462 L25AAXHX63262 H2590D.

Prepared for
Director
DEFENSE NUCLEAR AGENCY
Washington, DC 20305



Destroy this report when it is no longer needed. Do not return to sender.

UNCLASSIFIED

SECURITY CLASSIFICATION OF THIS PAGE (When Data Entered) READ INSTRUCTIONS REPORT DOCUMENTATION PAGE BEFORE COMPLETING FORM 2. GOVT ACCESSION NO. 3. RECIPIENT'S CATALOG NUMBER DNA 4240F PE OF REPORT & PERIOD COVERED IONOSPHERIC IRREGULARITIES: OPTICAL SUPPORT, Final Report for Period OF HAES SCINTILLATION EXPERIMENTS. 15 Dec 75 - 31 Jan 77 8. CONTRACT OR GRANT NUMBER(s) AUTHOR(s) DNA 001-76-C-0182/ Robert D. Sears 10. PROGRAM ELEMENT, PROJECT, TASK AREA & WORK UNIT NUMBERS 9. PERFORMING ORGANIZATION NAME AND ADDRESS Lockheed Palo Alto Research Laboratory 3251 Hanover Street NWED Subtask L25AAXHX632-62 Palo Alto, California 94304 11. CONTROLLING OFFICE NAME AND ADDRESS 31 January 197 Director Defense Nuclear Agency Washington, D.C. 20305 90 14. MONITORING AGENCY NAME & ADDRESS(if different from Controlling Office) 15. SECURITY CLASS (of this report) UNCLASSIFIED 15a. DECLASSIFICATION/DOWNGRADING SCHEDULE Approved for public release; distribution unlimited. 17. DISTRIBUTION STATEMENT (of the abstract entered in Block 20, if different from Report) 18. SUPPLEMENTARY NOTES This work sponsored by the Defense Nuclear Agency under RDT&E RMSS Code B322076462 L25AAXHX63262 H2590D. 19. KEY WORDS (Continue on reverse side if necessary and identify by block number) Electric Fields Auroral Intensity Precipitating Particle Energy Parameters Auroral Motions 20 ABSTRACT (Continue on reverse side if necessary and identity by block number) Photometric measurements of auroral spectral emission features and of the horizontal phase velocity of auroral motions were conducted at Chatanika, Alaska during several observing periods in 1976. These experiments provided ground-based optical support for the DNA HAES (High Altitude Effects Simulation) rocket experiments launched from Poker Flat. Data were obtained for the EXCEDE rocket flights of 28 February and 19 November as well as for the WIDEBAND coordinated rocket satellite experiment on 26 November 1976. net

DD 1 JAN 73 1473 EDITION OF 1 NOV 65 IS OBSOLETE

UNCLASSIFIED

SECURITY CLASSIFICATION OF THIS PAGE (When Data Enter

210118

SECURITY CLASSIFICATION OF THIS FAGE(When Data Entered)

20. ABSTRACT (Continued)

Additional experiments were conducted in coordination with the SRI/DNA incoherent scatter radar operation.

Multispectral data on the auroral emission intensities at 4278A and 6300A and the intensity ratio was analyzed in terms of the mean energy parameter for an assumed Maxwellian flux of precipitating electrons. Comparison between photometric determination of the mean energy parameter and that derived from incoherent scatter radar data provided a useful cross calibration of the two measurement techniques. This agreement also tends to confirm the theoretical predictions for the intensity ratio (R₆₄ 1(6300)/1(4278)) as a function of the mean energy parameter.

Additional analytical work was conducted to improve the three beam analysis code which allows inference of auroral E-fields and associated quantities from the auroral motion and intensity data. Results of the improved code are presented for the WIDEBAND rocket support experiment.

PREFACE

This is the final technical report on Contract DNA 001-76-C-0182 covering the period 15 December 1975 to 18 February 1977. The purpose of the research program reported herein was to determine the properties of the neutral and ionized consitituents in the auroral region by application of advanced optical sensing techniques in support of the DNA High Altitude Effects Simulation (HAES) experiments at Poker Flat, Alaska.

The experimental and analytical efforts were conducted at the Lockheed Palo Alto Research Laboratory and at the LMSC optical field site at Chatanika Alaska. The principal investigator on this program was Mr. R. D. Sears. Mr. D. E. Hillendahl also contributed to the program. We wish to acknowledge the support and assistance of Stanford Research Institute personnel at the Chatanika site, and the collaborative efforts of Drs. M. Baron and R. Vondrak of SRI. The support and encouragement of our colleagues at LMSC and of our DNA program officer, Dr. C. A. Blank are gratefully acknowledged.

	ON for
NTIS	White Section 🗹
DDC	Buff Section
UNANNO	INGED
JUSTICIO.	ATION
	HIGH/AVARABILITY CODES
Dist.	OF SPECIAL
Dist.	THE THE OF SPECIF

TABLE OF CONTENTS

			Page
PRE	FACE		1
1.	INTRODU	CTION	5
2.	SUMMARY	OF THE 1976 IONOSPHERIC IRREGULARITIES	9
	EXPERIM	ENTAL PROGRAM	
	2.1	Introduction	9
	2.2	Exploratory Experiments: 12 to 19 February 1976	9
	2.3	Excede ICE CAP, and WIDEBAND Rocket Support 20 February	11
		to 7 March 1, and 13 to 28 November 1976	
3.	THREE B	EAM DATA ANALYSIS CODE IMPROVEMENTS (NUWAV10)	14
	3.1	Introduction	14
	3.2	Code Improvements	14
	3.3	Examples of Improved Code Applications	17
		3.3.1 Statistical Parameters	17
		3.3.2 Wave Analysis Parameters	17
4.		NATION OF MEAN ENERGY PARAMETER FOR AURORAL PRECIPITATING	24
	ELECTRO	Introduction	24
		Photometer Measurements	26
		Comparison of Photometer and Radar Results	30
		Summary	35
5.	EXCEDE	ROCKET SUPPORT RESULTS	37
6.	WIDEBAN	D EXPERIMENT SUPPORT	40
	6.1	Introduction	40
	6.2	Latitudinal Distribution of Precipitation	40
	6.3	Measurements of Auroral Motions and Irregularities	. 1,1,
7.	SUMMARY	AND CONCLUSION	49
	7.1	Summary of Experimental Results	49
	7.2	Summary of Analytical Results	50

TABLE OF CONTENTS -- Continued

							Page
7.3	Ground-based	Optics	and	Future	HAES	Experiment	51
REFERENCES							54
APPENDIX A							57

1. INTRODUCTION

The DNA/LMSC ionospheric irregularities program is a continuing effort to apply advanced optical remote sensing techniques to support the DNA/HAES (High Altitude Effects Simulation) program. These techniques and the instrumentation used were developed under the nuclear test readiness program and have been refined and improved during ground based experiments supporting the HAES program rocket launches at Poker Flat, Alaska during the period of 1972 through 1976. Optical ground based support has been provided to the ICE CAP program (1972-1976), EXCEDE (1975-1976), COMMOCAP (1974), and WIDEBAND (1976) experimental programs over this period. Results of ground based optical measurements made in years preceding the current contract are described in references 1 through 10.

The ionospheric irregularities program seeks to define certain spatial and temporal variations (irregularities) in the properties of the upper atmosphere by means of sensing the spatial and temporal structure in visible and near infrared spectral emission features generated in the region of interest. The atmospheric variables which are measured and those which may be inferred from the measurements are summarized in Table 1. These measurements and the related analyses are described in detail in the references. Two specific types of photometric instruments have been developed for this program: a multispectral (3 color) photometer which measures the spectral intensity of atmospheric emissions in three separate spectral regions through a single field of view; and a multibeam (3 beam) photometer which measures a single spectral emission intensity in three closely spaced fields of view. References 1 and 2 contain a complete description of this instrumentation. In general, the multispectral photometer is used to determine the temporal fluctuations of spectral emissions over a wide spatial region, for example, over a meridional scan, whereas the 3 beam photometers detect the short term temporal fluctuations and medium scale spatial variations (10's of km). The instrumentation is operated at the LMSC optical research site at Chatanika which is co-located with the DNA/SRI incoherent scatter radar. Two types of observations have been made. During periods of no auroras, the 3 color photometer may be used to verify the absence of auroral precipitation to

support EXCEDE and other rocket experiments which require a minimum level of auroral activity. Also during quiet times, the three beam measurements of emission intensity from the OH, Na, and Ol species may be used to infer neutral winds and detect wavelike motions in the relevant emitting regions. During periods of active auroras the three color photometer is used in a meridional scan mode to determine the latitude distribution of auroral electron and proton precipitation intensity, the total energy deposited in the atmosphere by these species, and the mean energy parameter of the precipitating electrons. The three beam photometers are generally operated in the Ol emission wavelengths of 5577A and 6300A in order to provide data on E region auroral motions (from which E-fields are derived) and the F-region irregularity structure which may be related both to inhomogenieties in the precipitation source and the generation of ionized irregularities by plasma processes.

The ionospheric irregularity program has been geared to provide data from which two basic types of information can be derived: the physical processes which create irregularities in both the ionized and neutral media which then exhibited as structure in visible and/or infrared emission; and quantities which can be measured in the visible and/or near infrared which can be directly scaled from the natural atmosphere to the nuclear disturbed atmosphere. In either case, the data base for constructing and verifying predictive codes for nuclear burst disruption to various systems is expanded by such measurements.

This report presents the results of the ground based optical support experiments during 1976. Photometric measurements were made in support of the EXCEDE rocket experiment in February and in support of the WIDERAND coordinated satellite and rocket experiments during November. The ground based experiments and their specific relationship to HAES program objectives are summarized in section 2. Unfortunately because of weather and other problems, the ICE CAP series of rocket launches scheduled for February 1976 were postponed indefinitely. In addition to the specific rocket support observations made, a series of experiments related to expanding the capabilities of the multispectral and multibeam photometer observations was undertaken.

In addition to the experiments conducted at Chatanika during 1976 the analytical routines utilized to derive the wavelike properties of upper atmospheric motions and related quantities (see table 1) were improved significantly. These results are summarized in section 3. Section 4 contains a comparison of the SRI Untangle Code results with the optical determination of the mean energy parameter. We have shown, in collaboration with SRI, that both the total energy deposit and mean energy parameter derived by radar techniques and by optical techniques are self consistent and agree with theoretical predictions. These results have important implications with respect to utilization of optical techniques for determining effects of high altitude bursts upon the atmosphere, and the consequent systems effects, especially in the beta and debris deposition regions. Section 5 contains the results pertaining to the EXCEDE experiment and section 6 presents the preliminary results of our WIDEBAND support experiments. The summary and conclusions, section 7, contains an up-to-date assessment of the future utility of the ground based support optical experiments with respect to HAES program requirements.

TABLE 1

IONOSPHERIC IRREGULARITIES: PHOTOMETRICALLY MEASURED, AND INFERRED QUANTITIES

MEASURED QUANTITIES

A)	Photometric intensities vs. time in same field of view 1) 4278A N E-region 2) 4861A H "
	3) 5577A 0(ls) " 4) 6300A 9(lD) E & Fregion
В)	Photometric Intensities vs. time in three closely spaced fields of view 1) 4278A N ⁺ E-region 2) 5577A 0 ² (1S) " 3) 5890A Na " 4) 6300A 0(1D) E & F region 5) 7700-8100A, OH D-region
DERI	VED QUANTITIES
C)	Energy Deposit by precipitating particles (total), from Al Flux of precipitating protons , " A2

C)	Energy Deposit by precipitating particles (total)),	from Al
D)	Flux of precipitating protons	,	" A2
E)	Photometric intensity Ratios	,	" A4,A1
F)	Auto and cross spectra and related statistical quantities		" B
G)	Horizontal phase velocity of motions of emission	,	ıı F
G)	irregularities	,	1

INFERRED QUANTITIES

H)	Mean energy parameter of precipitating electrons ,	"	E
I)	Oxygen excitation and quenching chemistry kinetics,	11	A3, A4, E, F
J)	Spatial structure of optical irregularities ,	***	F
K)	Auroral electric fields	11	G,(Bl,B2)
L)	Pederson and Hall conductivities ,	"	C,D,E
M)	Joule heating in auroral regions ,	11	C, E, K
N)	Neutral winds and wavelike motions ,	11	F,G
0)	Frequency spectra of auroral E fields ,	11	G
P)	Large scale F-region structure	11	A4

2. SUMMARY OF THE 1976 IONOSPHERIC IRREGULARITIES EXPERIMENTAL PROGRAM

2.1 Introduction

Experimental operations of the photometric apparatus were conducted during two periods in 1976. During the February 10 to March 1 interval, observations were divided into two groups; those intended as exploratory measurements to extent the utility of the photometric techniques, and those oriented to direct support of EXCEDE and ICECAP rocket launches. The second period of operation, from 13 to 28 November supplied direct optical support to the WIDEBAND coordinated satellite and rocket experiments. The individual experiments which were conducted and their relationship to HAES program goals is summarized in the following sections. Table 2 digests the number of hours of data obtained with respect to each individual experiment.

It should be pointed out that the operational philosophy on the Ionospheric Irregularities program has been to obtain as much data relating to the specific experimental and analytical goals as is reasonably possible. Hence, photometric observations are normally made regardless of the rocket launch conditions as long as observing conditions permit. The experimental schedule is adjusted depending upon the rocket experiments which are counting down, and is also coordinated insofar as is practicable with the operation of the Chatanika incoherent scatter radar. The results of all of the following experiments are not discussed herein because limited financial sources did not allow adequate sampling and analysis of the large volume of data obtained, over 150 hours in 1976 alone.

2.2 Exploratory Experiments: 12 to 19 February 1976.

Experiment 1: E-field scans

This experiment was undertaken to determine whether auroral motions could be monitored at large off zenith angles such that E-fields could be inferred over a range of latitudes. We operated the 3-B-1 photometer at 5577\AA on the scan head which was set to operate on 30 degree angle increments at zenith, 30° N and 60° N zenith angles in the magnetic meridian. Photometer 3-B-2 was operated also on 5577\AA but at zenith. One additional goal of the experiment was to determine whether 30 second data periods could be used to

TABLE 2 IONOSPHERIC IRREGULARITIES: HAES – 1976 Operational Summary

	Fall Period	11/2	4	Wideband Rocket 1025 UT	0740-1120
		11/24		Systems Checks	Cloudy
		11/22	œ		0335-1030
		11/19		Excede Rocket 0406 UT	0325-1105
		11/15		Systems Checks	Cloudy
		11/14	-	H ₂ O Rocket 0318 UT	0215-0900
		3/7 20±	9		0600-1215
		3/1 19	4 6.	RICE Rocket 1046 UT	0505-1145
		18	14		0500-1230
		28	∞ *	EXCEDE + UTD Rockets 0547 & 1212 UT	0500-1250
		27 16	6 8 8		0500-1100
		26 15	m m		0520-1200
-		14	10 -1		0430-1220
		22 22	# 61		0500-1150
	Winter Period	12 21	12 12 13	+	0450-1250
		20	w w	+	0525-1310
		19	x .	+	0510-1356
		18	1.5	RICE Rocket 0706 UT [±]	0500-1300
		2.2	4 10	+	0500-1250
		16	e) io	+ + +	0535-1310
		15	-	+ + +	0645-1100
		4.0	×	+ + + +	0440-1305
		13	r-	+ +	0520-1300
		01 00	ь		0520-1220
		201	1+		0550-1300
		2/10	NO		0705-1255
1		Date/Tape No Experiment	1 E-Field-Scan 2 E Field Zentin 3 AW/AGW 4 D&E Winds 5 E&F Winds 6 EXCEDE 7 SWIN/SWIR/TMA 8 WIDEBAND (See No. 5 10t description)	Coordinated Rocket and Satellite Passes (known) ISIS TRIAD AR-C S3-2	Operating Hours (on data)

*Thata obtained in Exceed Support Mode. I Operations continued until 3/12 but no useful data were obtained because of cloudy weather.

infer E-fields instead of the 300 second periods previously used for this part of the experiment, the 3-B-1 scan dwell time was set at 30 seconds for each angle. Thirty second intervals taken at zenith will allow comparison directly between 3Bl and 3B2 results. We conducted this experiment in hopes of obtaining corroborative data from satellites S3-2 and Triad.

Experiment 2: E-field at zenith.

The data from 3B2 in experiment No. 1 will be used to infer E-field structure and temporal variations for comparison with Chatanika radar and satellite results.

2.3 EXCEDE, ICECAP, and WIDEBAND Rocket Support 20 February to 7 March 1, and 13 to 28 November 1976.

Photometer Configuration: Wavelengths as Before:

3 Color: Scan head

3-B-1: Zenith

3-B-2: Zenith

Experiment 3: AIW/AGW studies

Here, we hoped to measure wave-like events in the auroral precipitation as observed by photometer 3B2 and in the Na layer as observed at 5890A on photometer 3B1. Previous data indicates that a dispersive type of auroral motion spectrum is observed both in the auroral E-region and in the Na layer when ATW's are generated. We will coordinate these measurements with Wilson's ground based detection of auroral ATW's. Energy deposit by precipitating particles in the auroral E-region is monitored with the 3C scanning photometer and by the photometer 3B2 for Joule heating input. Large enhancements in total energy input such as on 10 March 1975 may create large AGW's which may manifest themselves as TID's at large distances from the auroral region. These wavelike motions may excite IR-active species at large distances from the auroral region.

*AIW: auroral infrasonic wave

AGW: acoustic gravity wave

†TID: travelling ionospheric disturbance

Experiment 4: D and E-region winds

During quiet periods, the three beam photometers will be operated on Na and OH wavelengths such that the winds and/or wave-like motions in the OH (85 km) and Na (95 km) regions can be monitored. These data will add to those obtained in 1975. Transport of excited IR-active species is important to the understanding of the spatial structure of IR emission.

Experiment 5: E and F-region winds

Simultaneous operation of the 3 beam photometers on the 5577Å and 6300 A emissions of Ol will allow inference of the winds and wave-like irregularities in the E and F-region in quiet periods, and of the E-region auroral motions and their effects upon the F-region irregularity structure and winds during active periods. We hope to be able to monitor F-region winds even during the presence of auroral disturbances. For WIDEBAND support, the 3 color photometer is operated in a meridional scan mode to provide precipitating particle total and characteristic energy values vs. latitude.

Experiment 6: Excede Background definition

The 3C photometer was operated in a scan mode in order to monitor background auroral emission during the EXCEDE shot. Photometers 3B1 and 3B2 were operated on 5890A and 5577A wavelengths respectively to detect the possible presence of wave-like disturbances in the neutral atmosphere in the Na and 01 emitting regions.

Experiment 7: SWIR/SWIR/TMA events (these shots not run)

The 3C photometer will be operated in a meridional scan mode to determine energy input to ionosphere from precipitating particles and to estimate the mean energy of the electrons. A time history is required. 3Bl will be operated on 5890A to obtain the winds in the 95 km region before, during, and after the events. Comparisons of the photometric data with the TMA trail will allow calibration of this photometric wind measurement technique. 3B2 will be run on 5577A wavelength in order to measure the energy deposit by

Joule heating in the vicinity of the rocket trajectory up leg. Auroral E-fields will also be inferred from these data. This experiment was postposed indefinitely.

3. THREE BEAM DATA ANALYSIS CODE IMPROVEMENTS (NUWAV10)

3.1 Introduction

The computer code used to process the three beam data such that the spatial and temporal variations in airglow and auroral emission may be interpreted in terms of neutral winds, auroral motions, wavelike phenomena, etc. has a variety of internal functions which are assigned to subroutines plus the control program. It became apparent that certain subroutine functions, especially the input/output routines were inadequate to handle the range of parameters required to describe the several different physical phenomena causing the measured fluctuations, hence improvements in the code to handle these parameters were instituted. The code improvements are described functionally in the next section and examples of the enhanced input/output capabilities are presented in the following section. A more detailed description of the function of the basic analytical code plus its important algorithms is contained in reference 3.

3.2 Code Improvements

The functional organization of the three beam analysis code involves statistical processing of three simultaneous digital time series as input data. These data are read off library copies of the field data records by the main program and the pertinent channels are placed in a data array. The processing steps are functionally described in figure 1. Here, the important statistical quantities which are computed are blocked out and the flow through the wave analysis section is displayed.

A major modification to the data input and control routing was made in order to compress successive five minute samples of data within the 300 unit sample length of the basic computation. Because successive intensity samples are recorded nominally every second, with a 300 second series making up one digital record, it was necessary to perform boxcar averaging on successive n units of data in each time series in order to obtain an overall compression factor of n. We have tested this aspect of the code up to a value of n = 12, i.e., a one hour interval of data compressed into the 300 sample time series. The consequencies of such compression of the data is a shifting of the frequency

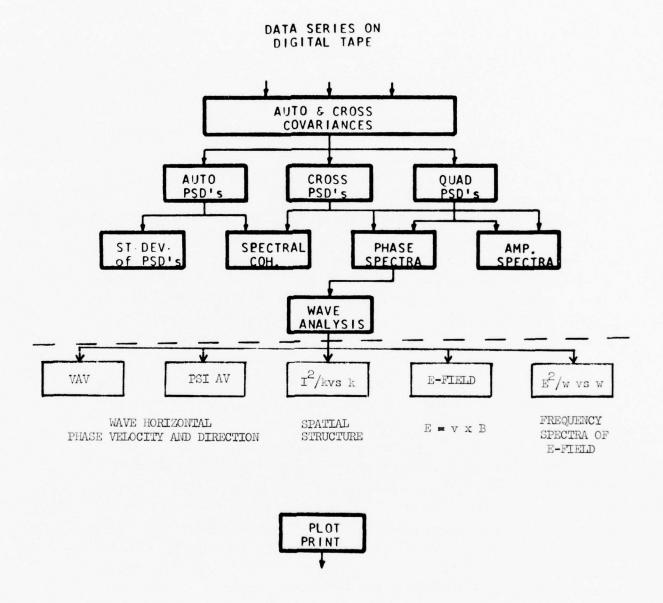


Figure 1 Flow diagram of computer program used to analyze three beam photometer data. The improved subroutines for obtaining average phase velocity, direction, etc. are those indicated below the dashed line.

window for the statistical and wave analysis parameters by a factor of 12. This frequency window shift hopefully will allow us to explore the dispersive effects of the Brunt-Vysala frequency and acoustic cut off region (around 0.003 Hz, 5 min period) upon wavelike phenomena in both the neutral atmospheric emission and in the motion of auroral excited species.

As the code previously existed, each of the statistical quantities was independently provided as both tabular and graphical output but little post processing on the wave analysis data was performed. The important functional modifications to the wave analysis code are described below the dashed line in figure 1. Here, the wave analysis output in terms of the wave phase velocity spectra are post processed to provide weighted averages of the three redundantly computed phase velocity spectra. The weighting function is derived from the coherence spectra such that pairs of time series exhibiting high coherence levels play a stronger role in the computation of average phase velocities than the channels exhibiting lower coherence. In addition to these outputs, the spatial spectra of the emission fluctuations are computed. This involves a simple coordinate transformation between the power spectral density data and the horizontal phase velocity at a given spectral frequency.

Because much of the interpretation of the three beam photometer data has been in terms of auroral motions and the E fields which may be inferred therefrom, we have included both tabular and graphical output of several quantities related to E fields, namely the equivalent E field geometrical components (vs. frequency) and a plot of the E field fluctuation spectrum separated into north-south, and east-west geomagnetic coordinates. Both of these outputs are useful when comparing auroral motion data and inferred E fields with other experimental measurements of the same quantities. Finally, the plot/print output routine was altered to conserve resources by combining plots of the same or closely related parameters on the same coordinate system. Although the major goal of the code improvement effort was to enhance the useability of the code, a minor improvement in running time was realized (approximately 20 seconds CPU time for each three channel record segment of 5 minutes duration) and the output volume in both plot and print formats was

reduced a factor of three.

3.3 Examples of Improved Code Applications

3.3.1 Statistical Parameters

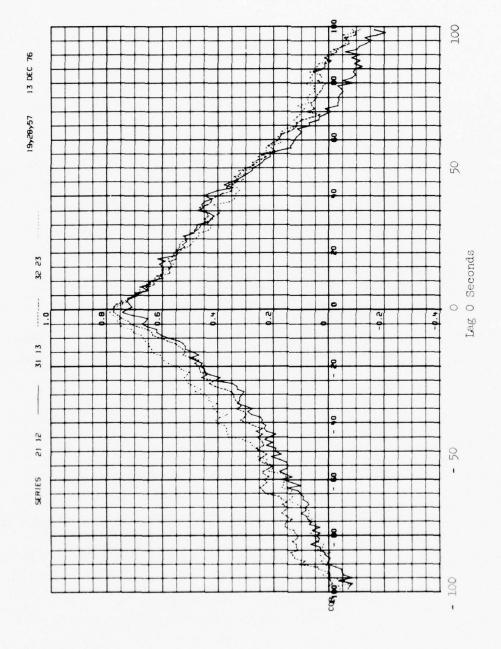
The major changes in the subroutines for plotting out the statistical parameters is reformatting them such that more than one parameter is provided per plot. The new formats for correlation function, and power spectral density plots are illustrated in figures 2 and 3, for periods of active auroras. The abcissa coordinates of the plots are now self adjusting such that when the spectral window is changed by the reformatting of data in the control program, the data are presented in the proper frequency coordinate window. Reformatted plotting of the other statistical parameters specified in figure 1 is similar to those illustrated herein.

3.3.2 Wave Analysis Parameters

The weighted wave velocity and directional spectra which are new outputs of the program are illustrated in figure 4. Here, one can readily detect wave dispersive velocity effects in both magnitude and direction.

For applications of the analyses to auroral motions and determination of the auroral E-fields, the equivalent E-field frequency spectra are printed out rather than plotted. The reason for this choice is that the selection of an equivalent E-field value is normally based upon either the lowest frequency point or the lowest velocity point, depending upon relative coherence levels and the shape of the phase velocity spectrum. The listing provides these values related to the geomagnetic coordinate system as E (north-south) and E (east-west). Fluctuations in equivalent E-field vs. frequency are directly relateable to other experimental measurements, however, and these spectra are plotted, again vs. geomagnetic coordinates, i.e., $E^2(N-S)/w$ vs. w and $E^2(E-w)/w$ vs. w. Sample cases of these spectra are presented in figure 5 a and b, for the same data interval as the previous examples.

The final wave analysis output which is plotted is the spatial frequency plot of the intensity fluctuations, I^2/k vs k. A typical plot of this



Plot of cross correlation vs. lag index for 3 beam photometer data. Figure 2

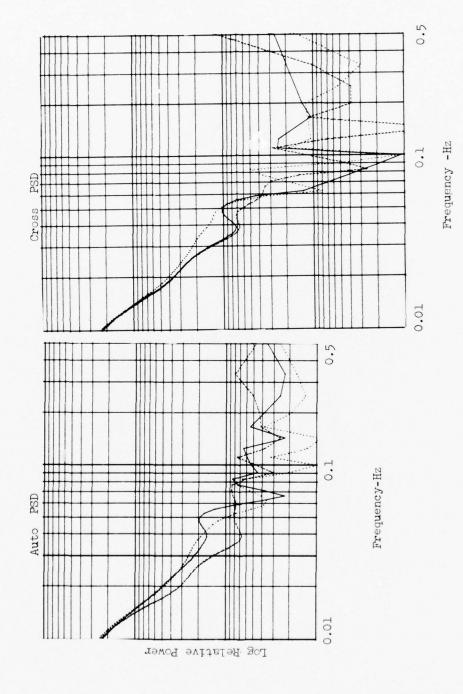


Figure 3 Auto and cross power spectral densities (PSD) revised plot format. Same data as figure 2.

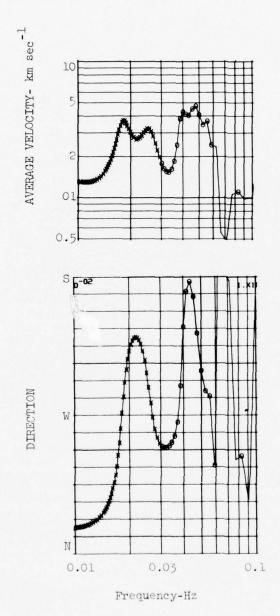


Fig. 4 Wave velocity and direction computed by weighted averaging of three sets of wave phase velocity vectors.

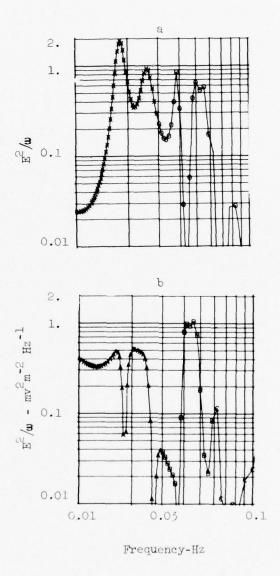


Figure 5 Electric field fluctuation spectra inferred from auroral velocity spectra of fig. 4. Curve A is N-S component; curve b is E-W component.

spectrum is illustrated in figure 6. Here, one notices the irregular behavior of this spectrum, and more surprisingly, the positive average slope vs. the expected negative slope. We have not run enough auroral motion data samples since the code improvement to determine whether this is an artifact of the coordinate change routine in the code or whether it is a real physical effect. The irregular nature of the spectrum can be removed by smoothing and by invoking weighting functions as was carried out in the computation of the average velocity parameters. Resources available to the program did not allow resolution of these problems, but they were not degradatory to the interpretation of the optical ground based support data for the various HAES experiments conducted this year.

The results of applying the improved wave analysis code to the various HAES experiments during 1976 are discussed in detail in later sections.

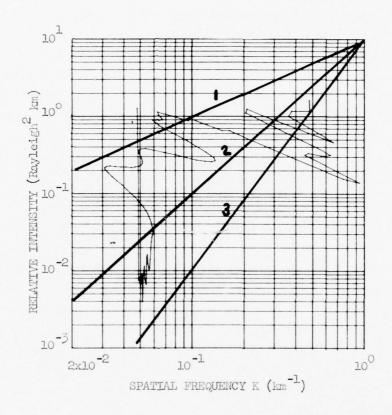


Figure 6 Spatial frequency spectra of auroral emission. Heavy lines denote \mathbf{k}^n spectrum where n = 1,2,&3.

4. DETERMINATION OF MEAN ENERGY PARAMETER FOR AURORAL PRECIPITATING ELECTRONS

4.1 Introduction

Systematic emission altitude variations in the relative intensities of auroral ionization source strength and of spectral emission features have been known since the early spectroscopic measurements of Vegard (see reference 11 for a discussion of the early work). These intensity variations are related to the mean energy of the precipitating particles because particles of different mean energy deposit the main portion of their energy at different altitudes depending upon the atmospheric density. Only in the past few years has it been possible to predict with confidence the altitude dependence of many important auroral spectroscopic emission features because of the complexity of the interactions between the particles of different energy distribution and pitch angle distribution with the atmosphere.

Theoretical models of the altitude dependence of N_2^+ 1st negative band emissions at 3914, 4278, etc. and of 01 forbidden emission features at 5577 and 6300A have been published by Kamiyama (12), Banks et al (13), Judge (14), and by Rees and Luckey (15). Of particular value to the interpretation of ground and aircraft based photometric observations is the predicted variation of the ratio $R_{64} = I(6300)/I(4278)$ as a function of the mean energy parameter for precipitating auroral electrons. The mean energy parameter α is one half the average energy if the energy distribution of the precipitating particles is assumed to be Maxwellian, i.e., $F(E) = F_0 E \exp\left(-E/\alpha\right)$. The assumptions and physical limitations of such multi-parameter models are discussed in detail in the references cited above. Their main limitations however, appear to be related to the errors caused by variations in atmospheric density vs. altitude from the model used, and by departure of the precipitating electron energy flux from a Maxwellian spectrum. Despite these potential sources of error, we show that the ration R_{6h} is a useful measure of the mean energy parameter.

Empirical relationship of the total energy deposit on the atmosphere by precipitating particles to spectroscopic emission intensities has been carried out by a number of investigators. For example, Wickwar et al (16) demonstrated that energy deposit derived from photometric measurements of the auroral

 $4278A\ N_2^+$ band intensity compared well with that derived from incoherent scatter radar measurement of the height profile of ionization. Because, the altitude variations of recombination coefficients in the auroral E-region as well as the fluorescence efficiency for production of the 4278A emission by incident particles now are both reasonably well known, these measurements not only provided a useful cross calibration of the radar and photometric measurement techniques, they also confirmed theoretical predictions. Additionally, comparisons (17) of rocket and satellite measurements of the incident electron flux total energy with photometric data also confirm the N_2^+ 1st negative band fluorescence efficiency values obtained in the laboratory.

Various attempts to confirm the theoretically predicted R(6300/4278) value have been made, but to date none have provided definitive confirmation of Judge's (14) or Rees and Luckey's (15) predictions over a wide range of auroral conditions. Mende and Eather (18) compared airborne photometric measurement on a rather weak aurora (100 R of 4278A emission) with satellite particle data obtained on OV1 18. Their single comparison was consistent with the Rees and Luckey prediction but cannot be considered definitive because the photometer field of view and the subsatellite geomagnetic field region did not physically intersect. Other comparisons have been made using rocket borne electron detectors, and on-board and ground based photometers, but the problems of non coincident experimental volumes and temporal and spatial fluctuations in auroral characteristics have precluded definitive confirmation of the ratio values, except perhaps for few special cases.

In this report section we describe the derivation of the mean energy parameter from optical observations of the R_{64} ratio value for two cases, observations at magnetic zenith, and observations in a meridional scan mode. These observations are then compared with coordinated observations made with the Chatanika incoherent scatter radar. The radar observations of electron density vs. altitude were analyzed in terms of the energy flux of the precipitating electrons by means of the SRI UNTANGLE code (19). The mean energy parameter for the precipitating electron flux is then compared with that obtained optically. This comparison provides an empirical cross calibration between the two measurement techniques, but more important, because the two techniques differ completely in their analytical basis, their quantitative

agreement tends to substantiate the theoretical predictions of R_{6l} vs. α .

4.2 Photometer Measurements

The three color photometer was operated in close coordination with the Chatanika incoherent scatter radar on several occasions during 1975 and 1976. Comparative measurements of the mean energy parameter are presented herein for two periods; 12 March 1975 during the Multi-rocket launch window, and 20 February 1976. During the 1975 Multi-support experiment the photometer and radar were both operated in meridional scan modes, but with asynchronous timing. During 20 February 1976 both the radar and photometer were operated with superimposed fields of view pointed at geomagnetic zenith.

Details of the operation of the photometer, calibration procedures, etc. have been described in previous publications. Pertinent photometer characteristics are summarized in Table 3.

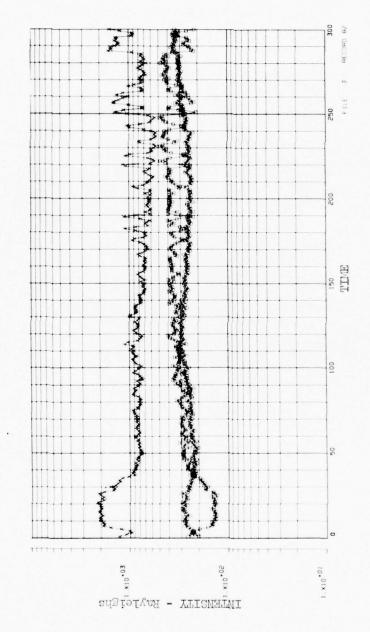
An example of the calibrated data output for the 20 February operational period is illustrated in figure 7. Here, the temporal variations in auroral intensity in the 4278A and 6300A spectral emissions and the contemporaneous ratio variations are plotted for a single five minute observing period (1 data record) on a second by second basis. The auroral intensity during this period exhibited only slow variations and the ratio variation was even smaller, indicating a nearly constant electron energy deposit and mean energy parameter vs. time for this period.

The mean energy parameter is derived from the R_{64} value by applying the Rees-Luckey relationship which is summarized graphically in figure 8. The curve simplified the theory in that the slight dependence of R_{64} upon total energy deposit (i.e., I(4278)) is not included in this curve, but the range of values for $0.1 \le \alpha \le 10$ kev is indicated by the bars. Because the normal auroral mean energy parameter ranges between about 1 and 10 kev., ignoring the total energy dependence causes an error in the estimated value of α from empirical values of R_{64} of only a few percent. In the next section, we compare the values of mean energy parameter obtained from the photometer technique with contemporaneous values obtained from application of the UNTANGLE code to the incoherent scatter radar observations.

TABLE 3
PHOTOMETER AND RADAR CHARACTERISTICS

Parameter	Photometer Value	Radar Value
Field of view	3°	0.40
Range resolution	none	6 km
Sensitivity*	> 1.0 Rayleighs (at 4278A)	> 10 ⁴ electrons/cm ³
Sensitivity* to ionization	on source in column > 0.005 erg/cm sec	> 2 x 10 ⁻³ erg/cm ² sec
Scan rates	2 deg/sec.	variable but usually slower
Scan increments	10 degrees (1975) 4 degrees (1976)	continuous
Integration times	1 second or longer	1-2 seconds and longer

^{*} Estimates based upon best conditions



Calibrated values of 4278 Å and 6300 Å intensities for 5 minute record period on 20 February 1976 and their ratios. X-indicates 4278 Å, 0-6300 Å, \square -RG4 ratio x 1000. Beginning time of record is 1155 UT.

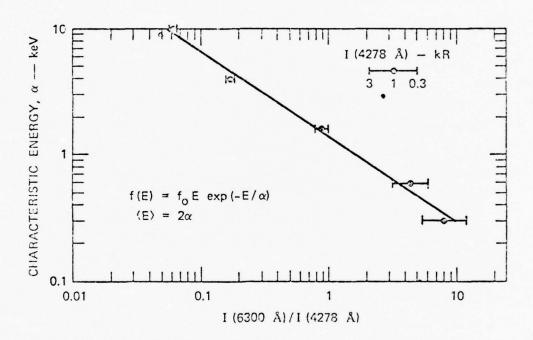


Figure 8 Characteristic energy parameter vs. intensity ratio $R_{64} = I(6300/I(4278))$ derived from Rees and Luckey theory in reference 15. The horizontal bars indicate the dependence of R_{64} on auroral intensity I(4278 Å).

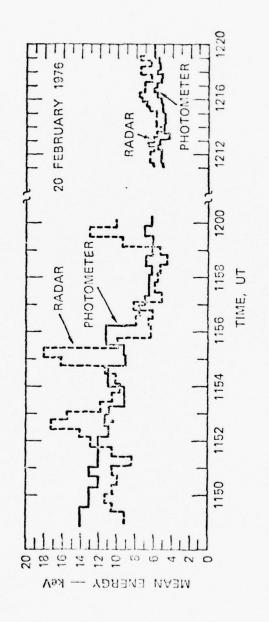
4.3 Comparison of Photometer and Radar Results

Coordinated observations were made on the night of 20 February 1976 with both the incoherent scatter radar and the photometer pointed at geomagnetic zenith. In order to understand the detailed comparisons of the mean energy parameter data, the pertinent characteristics of the photometer and radar are listed in Table 3. Active auroral conditions persisted during the entire observing period, 1040 to 1200 UT. After a substorm occurred at about 1110 UT, amorphous aurora covered the entire sky.

Figure 9 illustrates segments of the comparative measurements analyzed in terms of mean energy parameter. Both data sets were reduced with integration time of 20 seconds. Both data sets produced closely comparable results for the mean energy parameter except for a few unique periods when radar derived mean energies are much harder than those determined photometrically.

This effect is undoubtedly caused by the patchiness of the aurora such that the radar briefly observed a small scale hardening which was integrated out over the photometer field of view. These data as well as other comparable data obtained on 20 February are presented as a correlation plot in figure 10. Here, although some scatter is observed, most of the points agree within about 20 percent, which is within the mutual experimental errors of the two experimental techniques.

Scanning experiments were conducted during the 12 March 1975 Multi-rocket experimental period. During part of this period of coordinated observations, a bright arc was observed near zenith. Repeated scans through this arc region were made by both the radar and photometer, however, with asynchronous timing. Figure 11 illustrates the photometer scans through this region, showing the intensities of 4278A, 6300A, and R₆₄ intensity ratio vs. zenith angle. A comparable view of the arc is provided by the incoherent scatter data (provided by R. Vondrak, of SRI) in figure 12. The radar scans show the narrowness of the arc but do not provide as high temporal resolution of the arc's motions as the photometer scans. Unfortunately, during 1975 the meridional scan mode was operated with a 10 degree angle increment step, thus the spatial resolution across the arc is much poorer than that provided by the radar. Despite the discrepancies in measurement parameters and operational modes, we were able to obtain a number of period of comparable data,



photometric and radar data, 20 February 1976. Agreement between these independent techniques is good except for short periods when radar observes small scale hardening events which are unresolved to photometer. Time variation of mean energies for precipitating particles computed from Figure 9

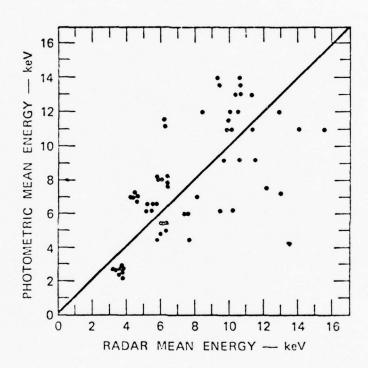


Figure 10 Correlation plot of comparative measurements of mean energy derived from photometric and incoherent scatter radar data for 20 February 1976. Each point represents a 30 second average. The cluster of points at low energy represents approximately 50 data points obtained during a period of constant energy input.

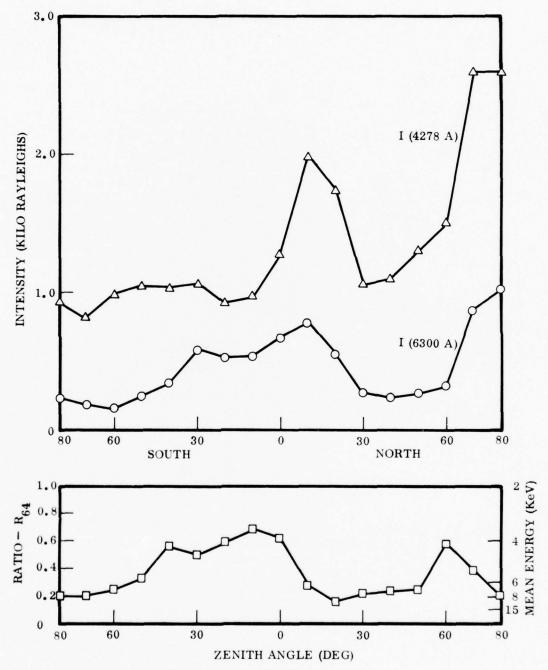


Figure 11 Calibrated photometer scans through arc region on 12 March 1975. Intensity of 4278 Å and of 6300 Å emission is plotted together with their intensity ratio, R_{64} . Note that for these data, the scan position increment was 10 degrees with a dwell time of 5 seconds at each position.

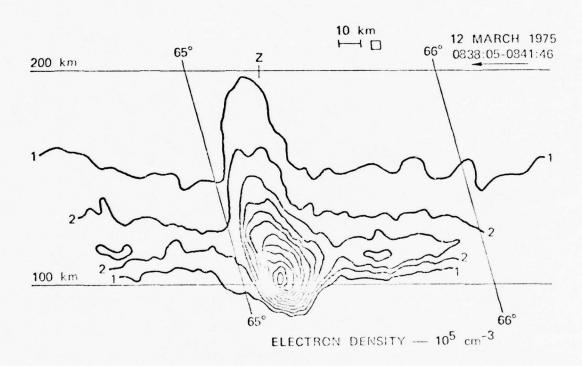


Figure 12 Contour map of electron density vs. height measured by the Chatanika incoherent scatter radar during a meridion scan. Contours are in units of 105/cm2 and are given in intervals of 1,2,4,5,6,8,10, etc. Data furnished courtesy of SRI.

i.e., when the photometer and radar were looking at the same portion of the sky at nearly identical times. Results of one such comparison are illustrated in figure 13. Here, the radar scan has been integrated over 10° angles to make its field comparable to the photometer. The fields of view generally coincided spatially within about 30 seconds. We see that the radar has outlined the energetic portion of the arc more adequately than the photometer, but both techniques produce closely comparable values of mean energy parameter in the diffuse precipitation region to the south of the arc. The moderate disagreement between the techniques at angles to the north of the arc are probably due to the differing geometry of the two measurements.

4.4 Summary

We have shown that the Rees and Luckey theory relating the mean energy parameter for precipitating electrons to the photometric R_{64} ratio agrees well with measurements of the mean energy independently derived from incoherent scatter radar measurements as analyzed by the UNTANGLE code. Such agreement provides cross calibration between the experimental techniques and furthurmore tends to confirm the predictions. Applications of these results to the WIDEBAND rocket launch is described in a later section.

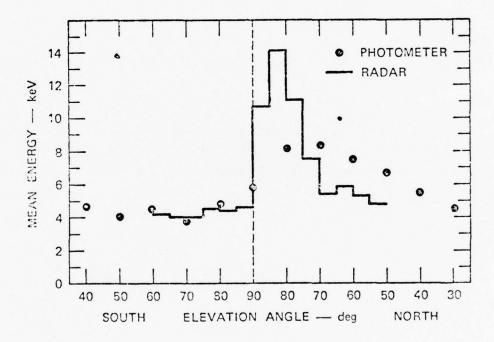


Figure 13 Comparison of mean energy for precipitating electron flux derived from radar and photometric measurements during scar operations in meridional plane. Data for 12 March 1975. Radar data are integrated over 10° scan angle to correspond with photometer angle increment setting. Narrow are near zenith was missed by the photometer.

5. EXCEDE ROCKET SUPPORT RESULTS

Excede rockets were fired on 28 February and 19 November 1976. Our support for these experiments was mainly limited to confirming that the launches occurred during low levels of auroral activity such that the electron gun excitation in the visible and infrared was not appreciably contaminated by ambient auroral ionization and emission processes.

Data was obtained in support of EXCEDE experiments by the three color photometer operated in a meridional scan mode. During the February operation scan angle increments were set to 10 degrees with a 5 second dwell time. During the November period, a scan angle increment of 4 degrees was chosen, with a 2 second dwell time. Both scan programs allowed a full scan between 10 degree elevation angles in 80 seconds, i.e. 2 degrees per second. We found that the advantage of the shorter integration time and smaller scan angle increment made up for the somewhat larger statistical error in calibrated intensities because smaller scale and/or shorter time features exhibited in aurora arcs could be defined better in the new scan program.

Figure 14 illustrates the photometric intensities vs. scan angle for the February EXCEDE event. It is clear that a low level of auroral activity existed on the upleg trajectory, although some activity is present to the north.

The November EXCEDE data are likewise presented in Figure 15. Again, the activity level is lower on the upleg trajectory. In both cases, it is apparent that the rocket shots were conducted early enough that the uplegs passed equatorward of the main part of the diffuse precipitation flux is low as well as the energy parameter, i.e. the maximum rate of auroral ionization is at higher altitudes than during active, discrete auroral arc displays. These are the conditions most conducive to successful EXCEDE experiments at Poker Flat and are readily identifiable by photometric meridional scan observations. It should be noted that our conclusions parallel those obtained from the Chatanika Incoherent Scatter Radar insofar as on site observations were compared.

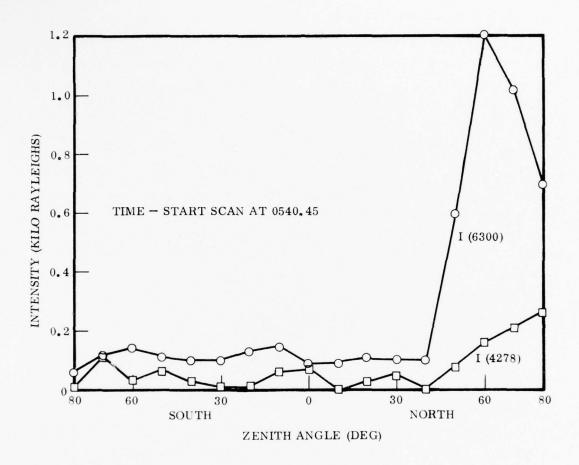


Figure 14 Meridional scan of 4278 Å and 6300 Å intensity for EXCEDE launch of 28 February 1976.

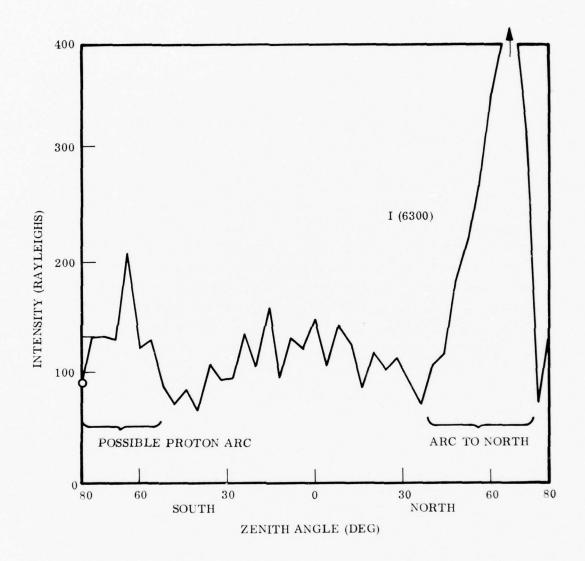


Figure 15 Meridional scan of 6300 Å intensity for EXCEDE launch of 19 November 1976. Intensity enhancement to south is probably caused by a diffuse proton arc. Noise in 4278 Å channel and low intensity level did not allow a meaningful plot.

6. WIDEBAND EXPERIMENT SUPPORT

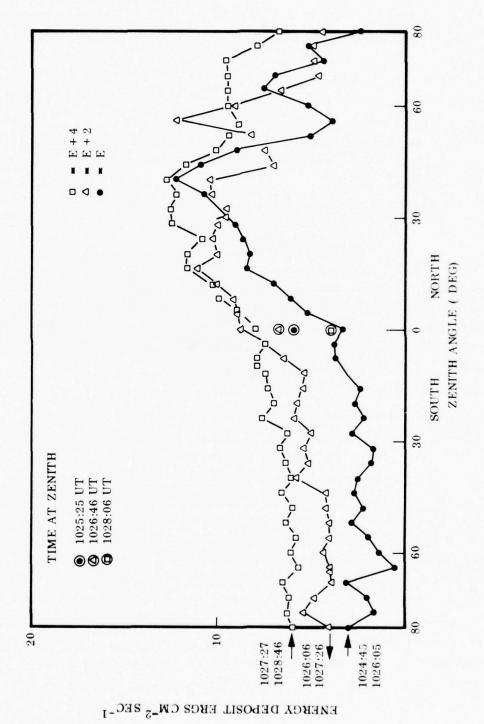
6.1 Introduction

WIDEBAND experiment support was provided by the meridional scanning three color photometer as well as two three beam photometers observing auroral motions at zenith. The meridional scanning photometer operated on wavelengths 4278A, and 6300A and provided data on total energy deposit in the atmosphere by precipitating particles, total flux of protons (4861A), and intensity of 6300A from OI, which provides the mean energy parameter when ratioed with 4278A as discussed in section 4. The three beam photometers were operated at 5577A and 6300A wavelengths in order to obtain auroral motion data as well as the F-region irregularity motion. The next section discusses the latitudinal distribution of total energy deposit by precipitating electrons and their mean energy parameter. The auroral E-fields are inferred from the 5577A three beam photometer data. Motions of the 6300A, F-region irregularities are presented but a full interpretation of these data is premature insofar as the physical mechanisms creating the observed irregularities and their motions are not fully defined.

6.2 Latitudinal Distribution of Precipitation

The three color photometer was operated in a meridional scan mode such that the latitudinal distribution of the intensities of 4278A, 4861A, and 6300A emissions could be determined during the WIDEBAND rocket launch period. As previously described, the 4278A intensity provides a direct measure of the energy deposit in the field of view by precipitating electrons and protons. The 4861A emission intensity provides a measure of proton particle flux into the atmosphere, and 6300A emission from OI provides a means of obtaining the mean energy parameter of the precipitating electrons as described in chapter 4. In this section, we describe the distribution of energy deposit which is a direct measurement of the ionization source strength, and the concurrent variations of the R_{64} ratio from which the mean energy parameter is derived. We have not reduced and calibrated the 4861A data as yet.

Three consecutive scans of the three beam photometer which were taken immediately after rocket launch at 1025UT are presented in figure 16. Here,

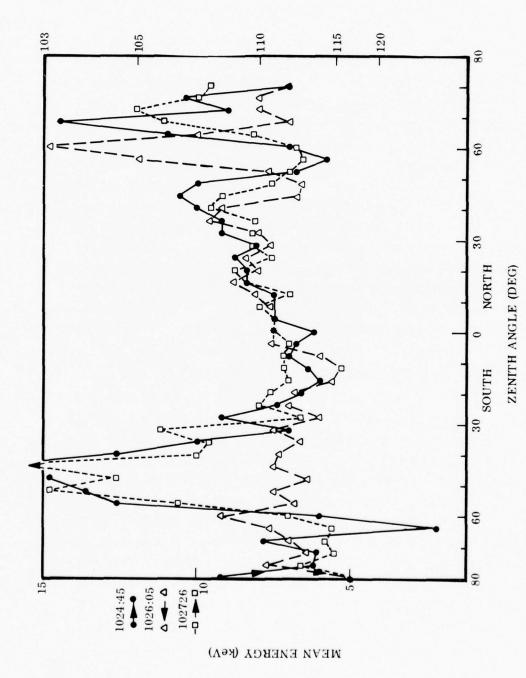


Latitudinal scan of total energy deposit as derived from h278 Å photometric intensities. Three scans during the flight of WIDEBAND rocket No. 2, 26 November 1976 are presented. Note that the zero level of successive scans indicated by Δ and \Box are offset by 2 and 4 ergs/cm² sec respectively to separate the curves.

Figure 16

the 4278A intensity vs. zenith angle is converted to the total energy deposited in the atmosphere. The direction and time duration of the scans is indicated on the figure. The zero level for energy deposit also has been shifted by 2 erg cm⁻² sec⁻¹ for consecutive scans in order to separate the curves for clarity. These data show that a weak ionizing flux was present to the south of zenith (approximately 1 to 2 erg cm⁻² sec⁻¹) gradually increasing in magnitude to zenith. Near zenith, the horizontal gradient in ionizing flux increased indicating that the diffuse precipitation region grows stronger to the north. At greater distances to the north, one or more discrete arcs are observed which is typical for the quiet time diffuse auroral region. It should be noted that in the diffuse precipitation region near zenith the overall intensity changes by nearly a factor of two from scan to scan, but the horizontal gradients appear to remain similar in form. This is clearly not an instrumental effect. Additionally, exemination of figure 16 shows that the discrete arc to the north also shifts not only in magnitude but in location as successive scans are made. However, this motion probably does not affect the data obtained on the rocket upleg (at about 10° north zenith angle) because it remains within the diffuse precipitation region.

The mean energy parameter computed from the R61 ratio value is presented in figure 17 in a format similar to figure 16. Here, the mean energy increases from a generally soft value in the south to harder, more energetic, values in the north. The discrete arcs show the hardest values of mean energy ranging from about 10 to 15 kev which is consistent with previous observations. An apparent very large mean energy parameter is indicated for some scans in the region of 40 to 60° south zenith angle. These anomalously large values we believe are produced by a geometrical effect which has not been removed from the analysis at this time. The effect is produced by looking out from the edge of the precipitation region wherein the observed 4278A emission is produced by precipitating electrons near 120 km, but the 6300A emission is produced in the F-region (above about 180 km) outside the region of precipitation. Because the F-region equatorward of the diffuse quiet time auroral zone is depleted of ionization at times much after sunset, the emission of 6300 by electron-ion recombination is greatly reduced consequently producing anomalously low values for the Rob ratio. Further improvements in our analytical codes will be



Latitudinal scans of mean energy of precipitating electrons as derived from the photometric intensity ratio $R_{GL} = I(6300/I(4278~\text{Å})$. The right hand scale indicates the approximate altitude of peak ionization for the precipitating electrons. Figure 17

required in order to remove such geometrical artifacts.

The overall behavior of the mean energy parameter vs. zenith angle is closely parallel to the total energy value variations. This suggests that over the diffuse auroral region at least, the total precipitating electron flux is nearly constant vs. latitude but the mean energy increases slowly going from equator to poleward edges. The detailed behavior of the mean energy and energy deposit also shows some small scale features which are apparently real, not statistical artifacts. Similar effects have also been observed in the incoherent scatter radar data. For example, there are optical indications that the small F-region "bubble" observed at zenith angles of approximately 40 degrees to the south is a precipitating particle feature, not a remnant of the daytime F-region. At this time the data have not been fully reduced, consequently we are unable to determine whether this feature might be caused by proton precipitation rather than soft electron precipitation. Further effort to resolve the details of the optical emission features and interpret them in terms useful to the WIDEBAND measurements is required.

6.3 Measurements of Auroral Motions and Irregularities

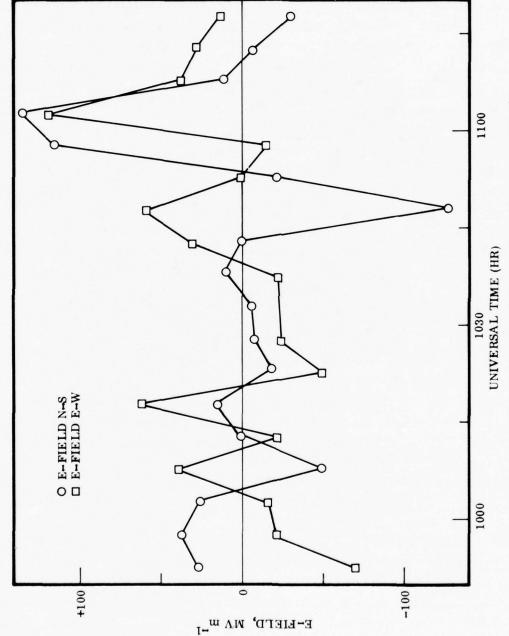
The three beam photometers were utilized to make auroral motion observations in the 5577A and 6300A emissions. The emission of 5577A in auroras is generated mainly by processes directly related to the auroral electron flux, hence irregularity motions observed in emission accurately depict the flux irregularities and their motion. The 6300A F-region emission however, is more complicated. The oxygen O(1D) state has a radiative lifetime of about 100 seconds, therefore excitation by auroral particles is integrated in time and smeared spatially due to neutral mass motions. An additional complication is the collisional quenching of the 1D state at altitudes below about 180 km, which effectively reduces the observed lifetime of the state. Because of these features, interpretation of the 6300A horizontal phase velocity and other associated quantities is made much more difficult.

Auroral motions observed in the 5577A emission region have been interpreted in terms of the E-fields required to generate the horizontal motions in precipitating particle flux irregularities, i.e., by the ExB forces. Electric

fields deduced by this technique for the period surrounding launch of the WIDEBAND rocket are depicted in figure 18. These E-field values are characteristic of a small region immediated around zenith and may not necessarily be identical to these in the region of the rocket trajectory. However, they probably provide a reasonable representation of the conditions in space which were sampled by the rocket. Additionally, the general behavior of the E-fields inferred photometrically agree qualitatively with the much larger scale fields as sampled by the Chatanika incoherent scatter radar, although the magnitudes appear to differ somewhat. The later term E-field variations, near 1100 UT apparently characterize the extremely large spatial shear in E-fields and auroral plasma motion observed both on satellited, by the Chatanika radar, and by WIDEBAND observations of irregularity motion. It is likely that the shear observed overhead at about 1100 UT is the later time development of shear motion observed at high latitudes during the rocket-satellite experiment at 1025 UT. which were reported by Livingston (private communication).

Observations of E and F-region irregularity motions made with the two three beam photometers are illustrated in figures 19 and 20. Here, the dispersive motion of the 5577A emission fluctuations depicts the auroral motion whereas the 6300A motions is a combination of auroral excitation and drifts of the emitting irregularities. These data are presented for the five minute period following rocket launch and therefore are representative of conditions at zenith averaged over the rocket flight time approximately.

In order to uniquely separate the effects of auroral motion from the neutral and ion motions representative of the observed fluctuations in the F-region, 6300A data, a much more intensive data reduction effort will be required. Qualitative comparisons of the 5577A and 6300A three beam photometer measurements of horizontal phase velocity and other parameters indicates that such an effort should be fruitful. If successful, then the 6300A data will be directly comparable to the WIDEBAND interferometer experiments and will be useful in interpreting these data.



Ionospheric Electric Fields computed from three beam measurements of auroral motions in 5577 Å spectral region for WIDEBAND rocket, 26 November 1976. Launch time 1025 UT. Figure 18

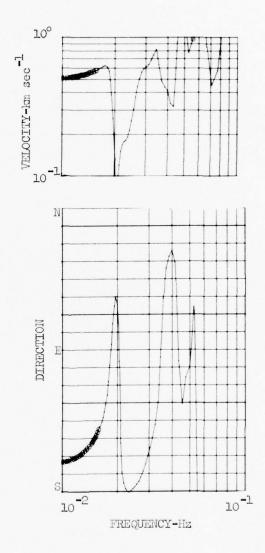


Figure 19 Velocity spectra for auroral motions observed in 5577 Å emission. Upper curve is dispersive velocity, lower curve is direction. Data for WIDEBAND satellite experiment, 26 November 1976.

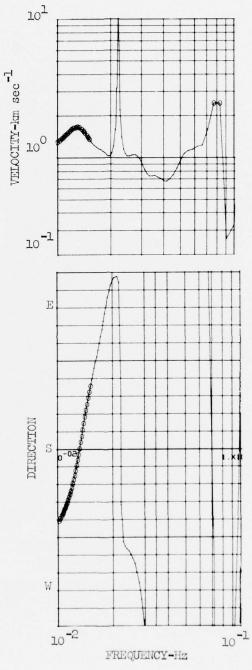


Figure 20 Velocity spectra for auroral motions observed in 6300 Å emission. Data are for WIDEBAND satellite experiment 26 November 1976. Format is similar to Figure 19.

7. SUMMARY AND CONCLUSIONS

7.1 Summary of Experimental Results

The Ionospheric Irregularities Program provided ground based optical supporting measurements to the DNA/HAES Program in Alaska for a number of rocket experiments conducted during the 1976 contract period. Specific rockets which were supported were:

•	EXCEDE	28 February 1976
•	EXCEDE	19 November 1976
•	WIDEBAND	26 November 1976

In addition, ground based support was operated for the ICECAP rocket series which was postponed indefinitely from the February window. These shots were the SWIR/SWIR/TMA series.

The principal results for the EXCEDE rockets were obtained utilizing the meridional scanning three color photometer. The purpose of these measurements was to confirm that a low level of precipitating flux background existed during the EXCEDE flights. Our results indicated that for both flights, although some auroral precipitation activity was present to the north, an acceptably low level of precipitation input was present during the flight at least in the vicinity of its upleg trajectory. The very small degree of precipitation present in the vicinity of the upleg trajectory was diffuse and apparently low in mean energy.

Data obtained in support of WIDEBAND are quite extensive and require much more interpretation than has been conducted to date. We observed a meridional gradient in both total energy deposit and in mean energy parameter during the 26 November coordinated WIDEBAND satellite-rocket experiment. Diffuse visible auroras extended to near zenith from the north indicating that an ionization gradient should exist near zenith. The scanning photometers expanded on this observation and quantified it. Small scale features in both E- and F-region structure observed by the incoherent scatter radar were also observed photometrically and indications of structure in the precipitating flux as well as in the ambient ionosphere were verified. The three beam photometer data on auroral E-fields showed a generally low level, but temporally dynamical E-field behavior.

These data agreed well with the radar. F-region structure and motions as observed in the 6300A OI emission line were very complicated. Dispersive motion was observed wherein the horizontal phase velocity varied significantly in magnitude and direction with frequency. These data also agree qualitatively with the WIDEBAND satellite interferometer receiver data (Livingston et al, private communication) although we have not been able to carry out detailed quantitative comparisons as yet. The WIDEBAND support data require much more effort in reduction and interpretation if they are to be quantitatively useful in analysis of the ionospheric properties which produce the observed scintillation effects on WIDEBAND.

7.2 Summary of Analytical Results

Analytical efforts during the 1976 Ionospheric Irregularities Program were confined to improvement of the three beam data reduction code and to confirming the cross calibration between photometer and incoherent scatter radar measurements of the mean energy parameter of the precipitating electron flux. Code improvements will allow much more flexible use of the three beam photometer technique for measurements of auroral motions, neutral winds and wavelike motions, and their associated quantities.

Perhaps the most important analytical results obtained during 1976 was the cross calibration of photometric and incoherent scatter radar techniques for measurement of the precipitating electron flux mean energy parameter. Theoretical results indicated that for Maxwellian energy distribution in the precipitating electrons, the ratio of emission intensities $R_{64} = I(6300)/I(4278)$ would be a useful measure of the mean energy parameter. Comparisons of the photometric data with equivalent quantities computed via the SRI/UNTANGLE code using incoherent scatter radar data provided a cross calibration between the experimental techniques as well as confirming the theoretical predictions.

This result is important because it will allow use of either photometer or radar measurements of both energy and mean energy parameter in future HAES experiments with more confidence as well as provide additional comparative data for past and/or future nuclear test measurements.

7.3 Ground-based Optics and Future HAES Experiments

Passive ground-based optical support experiments have been limited to detection of the optical emission features from limited altitude regimes characteristic of the emitting species. The Ionospheric Irregularities Program has concentrated upon the well known auroral and airglow emitting species which are listed below:

Species	Wavelength	Altitude of Peak Intensity
ОН	near IR and IR	85 km
Na	5896A	95 km
OI	5577A	95 to 120 km
OI	6300A	150 to 300 km
N 1	4278A	90 to 150 km

These spectral emission features and their altitude dependences are now reasonably well known, and the features can be interpreted in terms of their causitive phenomenology with confidence. Likewise, application of HAES measurements of the temporal, spatial, and spectral characteristics of these features to further understand the existing high altitude nuclear effects data base is theoretically and analytically supportable. However, we must consider other equally important spectral emission features; for example, emission from $\mathbf{0}_2$ in the atmospheric and infrared atmospheric bands, emission from NO, $\mathbf{N0}_2$ and other infrared active species, and emission from high altitude ionic species such as OII $(\mathbf{0}^+)$. Support of future HAES experiments will require such an expansion of the experimental capabilities in order to extend the altitude range accessible to ground- and/or aircraft-based optical support experiments.

In addition to extending the spectral range of optical support experiments, the spatial and temporal dynamical ranges must be extended by means of more flexible instrumentation design. For example, our present three beam photometer experiments are designed to measure auroral and neutral species motions over spatial scales of tens of kilometers. It is now well known that the spatial irregularities which cause scintillation effects, possible infrared irregularities,

and upper atmospheric turbulence scales extend down to the tens of meters sizes or smaller. Thus, it is incumbent that the ionospheric irregularity instrumentation be extended in capability to cover these scale sizes.

Results obtained to date on the Ionospheric Irregularities Program indicate that further valuable support can be provided to the HAES effort in the following areas:

INFRARED PROGRAMS

Ground-based infrared measurements of NO fundamental and overtone band radiances utilizing ultranarrowband interference filter radiometry

Measurements of energy input processes made by combined ground-based optical and incoherent scatter radar experiments

Measurements of transport processes made by combined optical and radar techniques

• SATELLITE AND RADAR PROPAGATION EFFECTS

Ground-based optical and scatter radar measurements of plasma properties, especially neutral and ionic motions, plasma gradients, and electron and ion temperatures, both in auroral and equatorial regions

High resolution optical measurements of auroral precipitation and plasma irregularities

High resolution optical and radar measurements of equatorial region plasma irregularities, especially those in the F-region

• NUCLEAR BURST PHENOMENOLOGY

Much interpretative data regarding the burst phenomenology at low latitudes must be obtained if it is to be applied to high latitude battle space conditions. Data regarding neutral and ionospheric wave motions, plasma drifts and irregularities, and other phenomenology conditions must still be obtained in order to fully utilize the existing nuclear test

data base. Optical measurements, especially those related to F-region irregularity generation will be valuable. Most of these are obtainable as supporting efforts for other ad-hoc experiments

In conclusion, it is especially important to point out the value of conducting well coordinated experiments utilizing a variety of observational tools. For example, the continued cooperative experimental and analytical efforts between the Ionospheric Irregularities Program and various programs conducted by SRI utilizing the Chatanika incoherent scatter radar have led to valuable insights into upper atmospheric and auroral phenomenology and its application to the HAES Program. Further efforts of this nature should be strongly encouraged.

REFERENCES

- 1. Sears, R. D., "Coordinated Measurements of Ionospheric Irregularities: Digital Photometer Design and Development," Topical Report, Contract DASA 01-71-C-0158, LMSC/D311213, Oct. 20, 1972
- 2. Sears, R. D., "Definition of Energy Input: Operation ICE CAP," Final Report, Contract DNA 01-72-C-0134, DNA 2985F, LMSC/D311131, Oct. 1, 1972
- 3. Sears, R. D., "Ionospheric Irregularities: Alaska Photometric Measurements," Final Report, Contract DNA 001-73-C-0110, DNA 3235F, Dec. 4, 1973
- 4. Sears, R. D., Evans, J. E., and Varney, R. N., "ICE CAP Analysis:

 Mechanisms for Energy Deposit in the Auroral Ionosphere," Interim Final
 Report on Contract DNA 001-73-C-0224, DNA 3293F, Jan. 15, 1974
- Sears, R. D., "Ionospheric Irregularities: Auroral Motions and Plasma Drifts," Final Report, Contract DNA 01-74-C-0179, DNA 3514, LMSC/D405729, Sept. 30, 1974
- Sears, R. D., "ICE CAP Analysis: Energy Deposit and Transport in the Auroral Ionosphere, ICE CAP 73-74," HAES Report No. 5, Final Report DNA 01-73-C-0224, DNA 3566F, Nov. 15, 1974
- Sears, R. D., "Versatile Family of Modular Aurora and Airglow Photometers," Appl. Optics 12, 1349-1355, 1973
- 8. Sears, R. D., "Intensity Correlations of the 4278\AA N $_2^+$ (0-1) First Negative Band and 5875\AA Emissions in Auroras," J. Geophys. Res. 80, 215-217, 1975
- 9. Sears, R. D., and Evans, J. E., "Coordinated Optical and Radar Measurements of Auroral Motions and Ionospheric Plasma Drift in Atmospheres of the Earth and Planets," Ed. B. M. McCormac, D. Reidel Pub. Co., 1974
- Sears, R. D., "Ionospheric Irregularities, HAES Program Support," HAES Report No. 29, Final Report, Contract DNA001-75-C-0098, 30 Sept. 1975
- 11. Chamberlain, J. W., Physics of the Aurora and Airglow, pp. 128-132, Academic Press, New York, 1961

- 12. Kamiyama, H., The Dependence of the Relative Intensity of some of the auroral Lines upon the Energy Spectrum of Precipitating electrons, Science Reports of the Tohoku University, <u>18</u>, 8390, 1967
- 13. Banks, P. M., Chappel, C. R., and Nagy, A. F., "Spectral Degradation, Backscatter, Optical Emissions, and Ionization," J. Geophys. Res. 79. 1459-1470, 1974
- 14. Judge, R. J. R., "Electron Excitation and Auroral Emission Parameters," Planet. Space Sci. 20, 2081-2092, 1972
- 15. Rees, M. H., and Luckey, D., "A New Model for the Interaction of Auroral Electrons with the Atmosphere," J. Geophys. Res. 79, 5181-5186, 1974
- 16. Wickwar, V. B., Baron, M. J., and Sears, R. D., "Auroral Energy Input from Energetic Electrons and Joule Heating at Chatanika," J. Geophys. Res. 80, 4364, 1975
- 17. These data are summarized in DNA, Reaction Rate Handbook, ed. M. H. Bortner and T. Baurer, Chapter 9, pp. 9-24 to 9-29, DNA1948H, March 1972. Published by DASTAC
- 18. Mende, S. B., and Eather, R. H., "Spectroscopic Determination of the Characteristics of Precipitating Auroral Particles," J. Geophys. Res. <u>80</u>, 3211-3216, 1975
- 19. Vondrac, R. R., and Baron, M. J., "Radar Measurements of the Latitudinal Variation of Auroral Ionization," Radio Science 11, 939-946, 1976

Appendix A Chatanika 1976 Data Synopsis Sheets

Tape: WOLFØ1 (60992-FILE 1)

<u>Date</u>:2/10/76 <u>Time</u>: 0600 to 1327 OT

Photometer(s): 3B1, 3B2, 3C

General Activity:

Active forms visible from before 0800 to after 1200

Operating Modes:

0647 to 1257-3c-4278, 4861, 6300, zenith 0657 to 1257 3B1 - 5890Å - zenith 0707 to 1257 3B2 - 7700 - zenith

Notes:

3/4 Moon -OH - NA Program 3B1-E channel very noisey

Tape: WOLF 02 (60992-FILE2)

Date: 2/11/76 Time: 0515 to 1330 UT

Photometer(s): 3B1, 3B2, 3C

General Activity:

Active after 0800 to about 1100 UT

Operating Modes:

0550-1300 3Bl on 30 sec dwell, 30 degree incremented SCAN mode (Denote

SCAN E) limits zenith 150° N (30° el. angle). 5577\AA

0550-1300 3B2 - 5577-zenith

0550-1300 3C - zenith

Notes:

Strong moonlight.

<u>Tape</u>: WOLFØ3 (60992-FILE 3)

Date: 2/12/76 Time: 0445 to 1250 UT

Photometer(s): 3B1, 3B2, 3C

General Activity:

Low-Auroral arcs detected to north

Operating Modes:

0520 - 1220 - 3B1 - 5577Å - SCAN MODE

0520 - 1220 - 3B2 - 5577Å - zenith

0520 - 1220 - 3C - zenith

Notes:

Strong moonlight

Tape: WOLFØ4 (60992 - FILE 4)

<u>Date</u>: 2/13/76 <u>Time</u>: 0450 to 1330 UT

Photometer(s): 3B1, 3B2, 3C

General Activity:

Strong near 1200 UT at zenith

Operating Modes:

0520 - 1045 3B1 5588Å, at 155° NL (25° N elevation)

1045 - 1300 3B1, 5577Å, SCAN E Mode

0520 - 1300 3B2, 5577Å, zenith

0520 - 1300 3C, zenith

Notes:

Moon Up

Satellite Passes:

0515 UT AE-C

0932 UT TRIAD

<u>Tape</u>: WOLFØ5 (61179-FILE 1)

Date: 2/14/76 Time: 0400 to 1335 UT

Photometer(s): 3B1, 3B2, 3C

General Activity:

Low most of evening

0800 Faint are to north

1100 Intense Ω form extending to zenith

1130 Back to Low activity

Operating Modes:

0440 - 1305 3B1, 5577Å, SCAN E Mode

0440 - 1305 3B2, 5577Å, Zenith

0440 - 1305 3C, zenith

Notes:

Full Moon

Satellite Passes:

0516 AE-C

0741 83-2

0902 TRIAD

1042 TRIAD

1218 ISIS-1

Tape: WOLFØ6 (61179 - FILE 2)

Date: 2/15/76 Time: 0600 - 1130 UT

Photometer(s): 3B1, 3B2, 3C

General Activity:

Quiet but very weak arcs to North

Operating Modes:

0645 - 1100 3B1, 5577Å, zenith

0645 - 1100 3B2, 6300Å, zenith

0645 - 1100 3C at zenith

Notes:

Satellite Passes:

0735 UT S3 - 2

1012 UT TRIAD

1149 UT ISIS1

After 1040 Cirrus moving in from south east.

1100 - Cloudy at zenith

1050 to 1130 3CR(ch 10) has abnormally hi CR- to 1010, 3Bl Weak wavelike variations.

0950 - 1000 (46) 3Bl ch 4 has noise, strong wavelike variations 3Bl, 3B2

Tape: WOLF\$\psi6\$ (61179 - FILE 2) Continued----

Notes: continued

0940 - 0945(44) 3B1(4) noise 0935 - 0945(43) 3B1(4) noise 0940 - 0945(42) 3B1(4) noise 0910 - 0945(38) 3B1(2) noise 0740 - 0835(30) 3B1, 3B2, 3C - occasional wavelike variations

Tape: WOLF 07 (61179 - FILE 3)

Date: 2/16/76

Time: 0500 to 1330 UT

Photometer(s): 3B1, 3B2, 3C

General Activity:

Quiet until 1030 UT

Active to north after 1030 but did not reach zenith.

Operating Modes:

0530 - 0929 0930 - 0950	3B1, 5890Å on zenith 3B2, 7700Å on zenith
0929 - 0930	3Bl and 3B2 on DCR
0950 - 1050	3B1, 5577Å, 155°N angle 3B2, 5577Å, zenith
1050 - 1315	3B1, 5577Å, 90 to 150° scans 30° increment 30 sec dwell 3B2, 5577Å zenith
0530 - 1315	3C on zenith

Notes:

Satellite Passes:

0542 - AE-C 0728 - S3-2 0942 - TRIAD

1120 - 1125 Ut 3CR erratic

Full Moon Period

0930 to 1050 3C noisey (ch 8 and 10)
1015 3C - ch 8 quieted down
1030 Activity in 3B and 3C9 at low level
1050 3C ch 8 noisey, ch 10 off scale

Tape: WOLF 07 (61179 - FILE 3) Continued --

Notes:

Check for possible proton arc after 0930

1115 (76) 3C very noisey all channels - 1125(78)

3Bl activity to north (30 $^{\circ}$ el angle)

1050 - 1200

1145(82) 3C (ch 10) zeroed 1200 - 1225 3Bl activity moved to 120° sector

Tape: WOLFO8 (61179 - FILE 4)

Date: 2/17/76 Time: 0430-1320 UT

Photometer(s): 3B1, 3B2, 3C

General Activity:

Quiet until 0850 0850 multiple faint arcs to zenith after 0900 strong activity from north to zenith

Operating Modes:

0500 - 0830	3B1, 5890Å, zenith 3B2, 7700Å, zenith
0835 - 1250	3B1, 5577Å, SCANS 90° to 150°, 30° angle increment, 30 sec dwell time
	3B2, 5577Å, at zenith
0500 - 1200	3C zenith

Notes:

Moon up after 0620 UT Satellite passes:

0721 - S3-2 0911 - TRIAD

Tape: WOLF09 (57930 - FILE 1)

Date: 2/18/76 Time: 0420 to 1330 UT

Photometer(s): 3B1, 3B2, 3C

General Activity:

0650 Faint glow to zenith, arc tonorth

0830 Very active

1230 Stable arcs to south

Operating Modes:

0500 - 0650 3B1, 5890Å, zenith

0820 - 1300 3B2, 7700Å, zenith

0650 - 0820 3Bl, 5577Å, SCAN mode 90° - 150°.

3B2, 5577Å

0500 - 1300 3C, zenith

Notes:

Satellite pass: TRIAD 1022 Rice Rocket launch: 0706:00

Tape: WOLF 10 (57930 - FILE 2)

Date: 2/19/76 Time: 0440 to 1320 UT

Photometer(s): 3B1, 3B2, 3C

General Activity:

Active all night

Operating Modes:

0500 - 1250 3B1, 5577Å, SCAN mode 30 $^{\circ}$ to 150 $^{\circ}$, 30 $^{\circ}$ angle increment, 30 sec dwell time

3B2, 5577Å, zenith

0510 - 1250 3C, zenith

Notes:

Satellite Pass: TRIAD, 0951 UT

Tape: WOLF 11 (57930 - FILE 3)

Date: 2/20/76 Time: 0510 to 1325 UT

Photometer(s): 3B1, 3B2, 3C

General Activity:

Active after about 0800 UT

Operating Modes:

0520 - 1310 3Bl, 5577, zenith

3B2, 6300, zenith

0525 - 1040 3C, SCAN mode, 10° -170 $^{\circ}$, angle increment 10° , 5 sec dwell time

3C, Magnetic zenith

Notes:

Satellite Pass: 0921 UT, TRIAD

Tape: WOLF 12(57930 - FILE 4)

<u>Date</u>: 2/21/76 <u>Time</u>: 0430 to 1310 UT

Photometer(s): 3B1, 3B2, 3C

General Activity:

Very active all night

Operating Modes:

0450 - 1100 1120 - 1250	3B1, 5577Å, zenith · 3B2, 6300Å, zenith
1100 - 1120	3B1, 5890Å, zenith 3B2, 7700Å, zenith for Loki Launch
0450 - 1250	3C. SCAN mode

Notes:

Sate:	llite Pa	ass:		TR.	LAD,	085	1	UT		
0730	Arc con	ning	up							
0815	Quiet									
0940	Strong	Arc	to	north	1					
1015	- 1030	Str	ong	N-S	for	ms,	Ω	form	to	zenith
			-	o wa						

Tape: WOLF 13 (61066 - FILE 1)

Date: 2/22/76 Time: 0430 to 1220 UT

Photometer(s): 3B1, 3B2, 3C

General Activity:

Some activity to north Quiet at zenith

Operating Modes:

0500 - 1144 3B1, 5890Å, zenith 0500 - 0917 3B2, 5577Å, zenith 0917 - 1144 3B2, 7700Å, zenith 0510 - 1144 3C, SCAN mode

Notes:

After 1120 UT, 3B2N has noise problem

Tape: WOLF 14 (61066 - FILE 2)

Date: 2/25/76 Time: 0400 to 1225 UT

Photometer(s): 3B1, 3B2, 3C

General Activity:

Hazy all evening
No auroras visible

Operating Modes:

0430 - 1220 3B1, 5890Å, zenith 0430 - 0630 0750 - 1220 3B2, 7700Å, zenith 0630 - 0750 3B2, 6300Å, zenith

0430 - 1220 3C SCAN mode

Notes:

Tape: WOLF 15 (61066 - FILE 3)

Date: 2/26/76 Time: 0450 to 1235 UT

Photometer(s): 3B1, 3B2, 3C

General Activity:

Active most of night after 0800

Operating Modes:

0521	-	1200	3Bl,	5890å,	zenith
0521	_	0840	3B2,	7700å,	zenith
0840	-	1200	3B2,	5577Å,	zenith
0621	_	1200	30	SCAN mod	de

Notes:

Data tape has 1 hr clock error before about 0520 UT

Possible proton arc before very active period

<u>Tape</u>: WOLF 16 (61066 - FILE 4)

Date: 2/27/76 Time: 0415 to 1130 UT

Photometer(s): 3B1, 3B2, 3C

General Activity:

Active arcs reach zenith after 0830 Breakup at 0905

Operating Modes:

0500 - 1100	3B1, 5890Å, zenith
0500 - 0830	3B2, 7700Å, zenith
0830 - 1100	3B2, 5577Å, zenith
0515 - 1100	3C, SCAN mode

Notes:

Gain problem on 3B2W at 0900

Tape: WOLF 17 (58817 - FILE 1)

Date: 2/28/76 Time: 0430 to 1305 UT

Photometer(s): 3B1, 3B2, 3C

General Activity:

Quiet through Excede launch, active later

Operating Modes:

0500 - 1250 3B1, 5890Å, zenith 3B2, 5577Å, zenith

3C, SCAN mode

Notes:

0546:40 Excede launch

212:50 UTD launch

1010 to 1020, 3BlE has gain problems

Tape: WOLF 18 (58817 - FILE 4)

<u>Date</u>: 2/29/76

Time: 0445 to 1235 UT

Photometer(s): 3B1, 3B2, 3C

General Activity:

Very active, auroras at zenith before 0430 UT

Operating Modes:

0500 - 1200

3B1, 5890Å, zenith 3B2, 5577Å, zenith 3C, SCAN mode

Notes:

3BlE channel erratic near beginning 3CR channel noisey, \sim 0730 to 0850, required gain changes

<u>Tape</u>: WOLF 19 (58817 - FILE 2)

Date: 3/1/76 Time: 0435 to 1200 UT

Photometer(s): 3B1, 3B2, 3C

General Activity:

Quiet until about 0730 Active to zenith later Sky hazy later

Operating Modes:

0505 - 0515	3B1, 5890Å, zenith
0740 - 1145	3B2, 5577Å, zenith
0515 - 0740	3B1, 5577Å, zenith
	2B2, 6300Å, zenith
0505 - 1145	3C. SCAN mode

Notes:

1045:45 Rice Rocket launch - very active to North

<u>Tape</u>: ETU Ø.1 (File 1, Tape # 57651)

Date:1-14-76

Time: 0150 to 0925 OT

Photometer(s): 3B1, 3B2, 3C

General Activity:

Quiet, clear skies until 0800 UT Hazy after 0830 UT

Operating Modes:

0215 - 0450 3B1, 3934Å; both at zenith 3B1, 5577Å 3B2, 6300Å 3C scan mode (10 to 170°, 4° increment, 2 sec dwell)

AZ Approx 45° true - To intercept H2O Cloud

Notes:

0318:19 Launch of H2O. Release at + 130 SEC. 3Bl developed HV short

Tape: ETU Ø2 (No copy made)

<u>Date</u>: 11-15-76 <u>Time</u>: 0330 to 1105

Photometer(s): 3B1, 3B2, 3C

General Activity:

No useful data - cloudy

Operating Modes:

Notes:

Ran system to check 3BlE tube, scan mode, etc.

Tape: ETO/3 (FILE 2, TAPE # 57651)

<u>Date</u>: 11-19-76 <u>Time</u>: 0315 to 1115 UT

Photometer(s): 3B1, 3B2, 3C

General Activity:

Clear skies

Diffuse aurora to zenith at 0830

Operating Modes:

0325 - 0810 3B1, 5890Å

0820 - 1105 3B1, 5577°

0325 - 1105 3B2, 6300Å

0325 - 1105 3C, SCAN MODE (10 - 170°, 4°, 2 Sec) MAG. Meridian

Notes:

0406:40 Excede Launch

0810 - 0815 3B1 on DCR and CAL

0415 - 0441 3C on DCR

1029 - 1 3C on DCR and CAL for 1 scan each

1030 - 1045 Reset DCR and CAL on 3C photometer

Tape: ETOØ4 (FILE 3 TAPE # 57651)

Date: 11-22-76 Time: 0335 to 1030 UT

Photometer(s): 3B1, 3B2, 3C

General Activity:

Clear sky - hazy near end Faint activity to North

Operating Modes:

0414 - 0924 3B1, 5577%, 3B2, 6300% 0934 - 1024 3C SCAN MODE (10 - 170°, 4°, 2 Sec)

Notes:

0603 - 0743 3CR problems

0743 - SCAN HEAD RESET - CHECK SCAN DATA BEFORE THIS TIME

Tape: ETU Ø5 (no copy made)

Date: 11/24/76 Time: 0215 - 1055 UT

Photometer(s): 3B1, 3B2, 3C

General Activity:

No useful data - cloudy later Possibly useful twilight run on 3934

Operating Modes:

System operated as check - see ETUØ1

Notes:

Tape: ETUØ6 (FILE 4, TAPE # 57651

<u>Date:</u> 11/26/76 <u>Time:</u> 0735 to 1130 UT

Photometer(s): 3B1, 3B2, 3C

General Activity:

Skies clear Activity built up, zenith band at rocket launch time

Operating Modes:

0740 - 1120 3B1, 5577; 3B2, 6300; 3C Scan mode (10 - 170°, 4°, 2 sec).

Notes:

1025:43 Launch of WIDEBAND - HI Rocket

1905 - 0910 all on DCR

0947 - 0952 3C on DCR and CAL, 1 sec each

1058(?) Scan head reset

DISTRIBUTION LIST

DEPARTMENT OF DEFENSE DEPARTMENT OF THE ARMY (Continued) Director Chief of Engineers Defense Advanced Research Proj. Agency Department of the Army ATTN: Fernand DePercin ATTN: LTC W. A. Whitaker ATTN: Nuclear Monitoring Research Deputy Chief of Staff for Ops. & Plans Department of the Army ATTN: DAMO-DDL, COL D. W. Einsel ATTN: Dir. of Chem. & Nuc. Ops. ATTN: Strategic Technology Office Defense Documentation Center Cameron Station 12 cy ATTN: TC US Army Ballistic Research Labs. ATTN: Tech. Lib., E. Baicy ATTN: John Mester ATTN: J. Heimerl ATTN: M. Kregl Director Defense Nuclear Agency Detense Nuclear Agency 2 cy ATTN: RAAE, Charles A. Blank 3 cy ATTN: TITL, Tech. Library ATTN: TISI, Archives ATTN: RAEV, Harold C. Fitz, Jr. ATTN: RAAE, Major John Clark ATTN: RAAE, Major James W. Mayo Commander US Army Electronics Command ATTN: DRSEL-PL-ENV, Hans A. Bomke ATTN: DRSEL Dir. of Defense Research & Engineering Department of Defense ATTN: S&SS (OS) ATTN: Stanley Kronenberg ATTN: DRSEL-RD-P ATTN: DRSEL-TL-IR, E. T. Hunter Commander ATTN: Inst. for Exploratory Research ATTN: Weapons Effects Section Defense Nuclear Agency ATTN: FCPR Commander US Army Foreign Science & Tech. Center ATTN: Robert Jones Livermore Division, Field Command, DNA Lawrence Livermore Laboratory ATTN: FCPRL Commander US Army Material Dev. & Readiness Command ATTN: DRXCD-TL ATTN: DRCCDC, J. A. Bender DEPARTMENT OF THE ARMY Commander/Director Atmospheric Sciences Laboratory US Army Missile Command US Army Electronics Command ATTN: DRSEL-BL-SY-S, F. E. Niles ATTN: R. Olsen ATTN: DRSEL-BL-SY-S, D. Snider ATTN: H. Ballard ATTN: DRSMI-ABL ATTN: Chief, Doc. Section ATTN: DRSMI-XS, Chief Scientist ATTN: CRDARD-OCS, Hermann Rob1 ATTN: CRDARD-P, Robert Mace Harry Diamond Laboratories 2 cy ATTN: DRXDO-NP, F. N. Wimenitz Commander US Army Nuclear Agency ATTN: MONA-WE, J. Berberet Navy Department ATTN: Code 461, R. G. Joiner ATTN: Code 461, Jacob Warner ATTN: Code 421, B. R. Junker Huntsville Office ATTN: ATC-0, W. Davies ATTN: ATC-T, Melvin T. Capps Dep. Chief of Staff for Research, Dev. & Acq. Department of the Army ATTN: NCB Division ATTN: DAMA-CSZ-C ATTN: DAMA-WSZ-C

DEPARTMENT OF THE NAVY (Continued)	DEPARTMENT OF THE AIR FORCE (Continued)
	Hq. USAF
Director	ATTN: DLS
Naval Research Laboratory	ATTN: DLCAW
ATTN: Douglas P. McNutt	ATTN: DTL
ATTN: Code 7701, Jack D. Brown ATTN: Code 2600, Tech. Lib.	ATTN: DLXP
ATTN: Code 7127, Charles Y. Johnson	ATTN: SDR
ATTN: Code 7700, Timothy P. Coffey	ATTN: Tech. Lib.
ATTN: Code 7709, Wahab Ali	
ATTN: Code 7750, Darrell F. Strobel	SAMSO/AW
ATTN: Code 7750, Paul Juluenne	ATTN: AW
ATTN: Code 7750, Klaus Hein	
ATTN: Code 7750, J. Davis	ENERGY RESEARCH & DEVELOPMENT ADMINISTRATION
ATTN: Code 7120, W. Neil Johnson	
ATTN: Code 2027, Tech. Lib.	Division of Military Application US Energy Research & Dev. Admin.
ATTN: Code 7750, Joel Fedder	ATTN: Doc. Con. for Major D. A. Haycock
ATTN: Code 7750, S. L. Ossakow	ATTN: Doc. Con. for Colonel T. Gross
ATTN: Code 7730, Edgar A. McClean	ATTN: Doc. Con. for Donald I. Gale
Officer in Charge	ATTN: Doc. Con. for David Slade
Naval Surface Weapons Center	ATTN: Doc. Con. for F. A. Ross
ATTN: Code WA501, Navy Nuc. Prgms. Off.	
ATTN: Code WX21, Tech. Lib.	Los Alamos Scientific Laboratory
ATTN: D. J. Land	ATTN: Doc. Con. for R. A. Jeffries
ATTN: L. Rudlin	ATTN: Doc. Con. for C. R. Mehl
	ATTN: Doc. Con. for G. Rood
Commanding Officer	ATTN: Doc. Con. for H. V. Argo
Naval Intelligence Support Center	ATTN: Doc. Con. for D. Steinhaus
ATTN: Document Control	ATTN: Doc. Con. for J. Judd
ATTN: Code 40A, E. Blase	ATTN: Doc. Con. for T. Bieniewski ATTN: Doc. Con. for D. M. Rohrer
	ATTN: Doc. Con. for D. M. Konfel ATTN: Doc. Con. for Martin Tierney
Superintendent (Code 1424)	ATTN: Doc. Con. for Marge Johnson
Naval Postgraduate School	ATTN: Doc. Con. for John S. Malik
ATTN: Code 2124, Tech. Reports Librarian	ATTN: Doc. Con. for William Maier
	ATTN: Doc. Con. for S. Rockwood
Commander Naval Weather Service Command	ATTN: Doc. Con. for Donald Kerr
Naval Weather Service Hqs.	ATTN: Doc. Con. for W. D. Barfield
Washington Navy Yard	ATTN: Doc. Con. for Reference Library
ATTN: Mr. Martin	ATTN: Doc. Con. for W. M. Hughes
ALLEN THE PROPERTY OF THE PROP	ATTN: Doc. Con. for E. W. Jones, Jr.
DEPARTMENT OF THE AIR FORCE	ATTN: Doc. Con. for John Zinn
	ATTN: Doc. Con. for E. A. Bryant
AF Geophysics Laboratory, AFSC	
5 cy ATTN: LKB, Kenneth S. W. Champion	University of California Lawrence Livermore Laboratory
5 cy ATTN: OPR, Alva T. Stair	ATTN: G. R. Haugen
5 cy ATTN: OPR, J. C. Ulwick	ATTN: A Kaufman
2 cy ATTN: OPR-I, R. Murphy	ATTN: A. Kaufman ATTN: D. J. Wuebbles
2 cy ATTN: OPR-I, J. Kennealy	ATTN: J. F. Tinney
AF Weapons Laboratory, AFSC	ATTN: Julius Chang
5 cy ATTN: SUL	ATTN: Tech. Info. Dept.
5 cy ATTN: DYT	ATTN: W. H. Duewer
ATTN: CA	
5 cy ATTN: DYM	Sandia Laboratories
ATTN: G. J. Fryer	ATTN: Doc. Con. for W. D. Brown
5 cy ATTN: DYC	ATTN: Doc. Con. for Org. 9220
	ATTN: Doc. Con. for Craig Hudson
Commander	ATTN: Doc. Con. for J. C. Eckardt
ASD	ATTN: Doc. Con. for C. W. Gwyn ATTN: Doc. Con. for D. A. Dahlgren
ATTN: ASD-YH-EX, Lt Col Robert Leverette	
	ATTN: Doc. Con. for M. L. Kramm ATTN: Doc. Con. for T. Wright
SAMSO/SZ	ATTN: Doc. Con. for Charles William
ATTN: SZJ, Major Lawrence Doan	ATTN: Doc. Con. for Sandia Rpt. Coll.
Lem La	ATTN: Doc. Con. for Doc. Con. Div.
AFTAC 5 cy ATTN: TD	
2 cy ATTN: Tech. Lib.	Sandia Laboratories
2 cy min. teen. bio.	Livermore Laboratory
	ATTN: Doc. Con. for Thomas Cook

ENERGY RESEARCH & DEVELOPMENT ADMINISTRATION

Argonne National Laboratory

Records Control

ATTN: Doc. Con. for A. C. Wahl ATTN: Doc. Con. for S. Gabelnick ATTN: Doc. Con. for J. Berkowitz

ATTN: Doc. Con for Lib. Services Rpts. Sec.

ATTN: Doc. Con. for Len Liebowitz

ATTN: Doc. Con. for David W. Green ATTN: Doc. Con. for Gerald T. Reedy

US Energy Research & Dev. Admin.

Div. of Hqs. Services

Library Branch G-043

ATTN: Doc. Con. for D. Kohlstad

ATTN: Doc. Con. for J. D. LaFleur ATTN: Doc. Con. for Class Tech. Lib.

ATTN: Doc. Con. for George Regosa

ATTN: Doc. Con. for Rpts. Section

ATTN: Doc. Con. for R. Kandel

ATTN: Doc. Con. for H. H. Kurzwek

OTHER GOVERNMENT AGENCIES

Department of Commerce

Office of Telecommunications Institute for Telecom Science

ATTN: William F. Utlaut

DEPARTMENT OF DEFENSE CONTRACTORS

Aero-Chem. Research Laboratories, Inc. 3 cy ATTN: A. Fontijn

AeroDyne Research, Inc.

ATTN: F. Bien ATTN: M. Camac

Aerospace Corporation

ATTN: Harris Mayer ATTN: Thomas D. Taylor

ATTN: R. Grove

ATTN: R. D. Rawcliffe ATTN: R. J. McNeal

University of Denver

Colorado Seminary Denver Research Institute

ATTN: Sec. Officer for Mr. Van Zyl ATTN: Sec. Officer for David Murcray

General Electric Company

TEMPO-Center for Advanced Studies 5 cy ATTN: DASIAC, Art Feryok ATTN: Warren S. Knapp

General Research Corporation

ATTN: John Ise, Jr.

Geophysical Institute University of Alaska 3 cy ATTN: Neal Brown ATTN: T. N. Davis

Honeywell Incorporated

Radiation Center

ATTN: W. Williamson

DEPARTMENT OF DEFENSE CONTRACTORS (Continued)

Institute for Defense Analyses

ATTN: Hans Wolfhard ATTN: Ernest Bauer

Lockheed Missiles & Space Company, Inc.

ATTN: John Kumer
ATTN: John B. Cladis, Dept. 52-12
ATTN: Billy M. McCormac, Dept. 52-54

ATTN: Tom James

ATTN: John James
ATTN: J. B. Reagan, D/52-12
ATTN: Martin Walt, Dept. 52-10
ATTN: Richard G. Johnson, Dept. 52-12
ATTN: Robert D. Sears, Dept. 52-14

Mission Research Corporation

ATTN: D. Archer ATTN: P. Fischer

Photometrics, Inc. ATTN: Irving L. Kofsky

Physical Dynamics, Inc. ATTN: Joseph B. Workman

Physical Sciences, Inc. ATTN: Kurt Wray

R & D Associates
ATTN: Robert E. LeLevier
ATTN: Forrest Gilmore

R & D Associates

ATTN: Herbert J. Mitchell

The Rand Corporation

ATTN: James Oakley

Science Applications, Inc.

ATTN: Daniel A. Hamlin

Space Data Corporation

ATTN: Edward F. Allen

Stanford Research Institute

ATTN: M. Baron ATTN: Ray L. Leadabrand ATTN: Walter G. Chestnut

Stanford Research Institute

ATTN: Warren W. Berning

Technology International Corporation ATTN: W. P. Boquist

Utah State University

ATTN: Doran Baker ATTN: Kay Baker ATTN: C. Wyatt ATTN: D. Burt

VisiDyne, Inc.